Integration of vanadium redox battery with PV systems: Modeling and simulation of Vanadium Redox flow batteries based on MATLAB/Simulink

Mohamed-Amine BABAY
Industrial engineering laboratory
Faculty of Science and Technologies,
Sultan Moulay Slimane University
Beni Mellal, Morocco
mdamine.babay@gmail.com

Mustapha ADAR
Industrial engineering laboratory
Faculty of Science and Technologies,
Sultan Moulay Slimane University
Beni Mellal, Morocco
Adar.mustapha@gmail.com

Mustapha MABROUKI
Industrial engineering laboratory
Faculty of Science and Technologies,
Sultan Moulay Slimane University
Beni Mellal, Morocco
Mus_mabrouki@yahoo.com

Abstract

Several models have been developed and they are now providing a good understanding of how VRB works. This knowledge is very important to evaluate its performance when applied in an electrical system. This article presents a new VRB model based an electrical equivalent model of VRFB, the effect of flow rate and pump power losses has been considered in modeling the VRFB. The VRFB is connected to a resistive variable load, for discharging and a system PV for charging. A control method for State of Charge (SOC) estimation is also proposed as it plays an important role in over-charge/discharge of VRFB. An equivalent electrical model of PV system including a VRB was implemented in MATLAB/Simulink environment to analyze the operational performance of the proposed system.

Keywords: Energy storage system, Vanadium Redox Flow Battery, State of Charge, Battery modeling, Solar PV, Flow rate

I. INTRODUCTION

Since the early 1970s, redox batteries have been extensively researched and several different redox pairs have been studied and reported in the literature. Only three of these systems have undergone some commercial development, namely the all-vanadium system (via VRB-ESS), the bromine-polysulphide system (RGN-ESS) and the zinc-bromine system (Powercell).

The vanadium bromine system has a high energy density so it can replace the all-vanadium system and can be used as an energy storage system for electric vehicles. Other redox flow battery systems due to slow electrochemical kinetics of redox torque, membrane fouling, cross contamination, high cost (mainly due to the membrane and battery design low efficiency), poor sealing, loss of bypass current and low and problematic energy capacity (due to the use of aqueous electrolytes). To date, one of the main factors limiting the further development of redox batteries is the high cost associated with ion exchange membranes.[1]

Alotto et al. [2]conducted a detailed study of the redox battery and described its development and future technical level. The first VRB model [3] parameterized the battery voltage, voltage loss, parasitic current loss, etc. [2]–[4]. But each of these studies is not effective in modeling the transient response, or is more complicated in the extended measurement of the parameters.

D'Agostino et al [5] tried to include the operating mode and start time in their VRB model and suggested that efficient management of electrolyte pumps would minimize losses and increase efficiency. Ontiveros and Mercado [6] proposed a new stacking model for VRB, which includes stacking efficiency and mechanical model to improve the accuracy of the VRB model and understand its operation. This paper implements a simplified VRB model that includes parasitic losses and takes into account the estimated voltage and state of charge of the battery in the solar system. The future energy system must be carefully designed to ensure energy reliability and security without being affected to insure the dynamic sustainability of the grid system.

Due to the intermittent nature of renewable systems, increasing permeability poses a huge challenge to the operation of the power grid.

However, due to growing global awareness of pollution and ozone depletion, most countries have chosen green energy policies, forcing technology providers to seek options for using and managing renewable energy without compromising grid supply and security.

The Energy Storage System (ESS) has become an indispensable partner for renewable energies, as it enables energy to be stored when it is available and supplied when the load requires it.

Many forms of energy storage have been developed, but the Battery Energy Storage System (BESS) is the most mature and developed technology in decades [7].
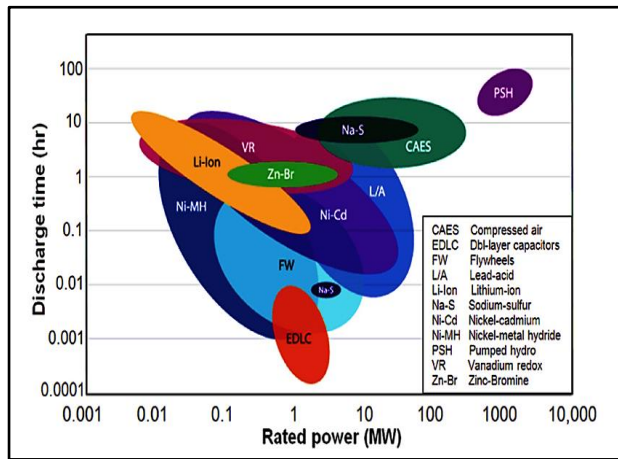
Figure 1:Power ratings and discharge times of various energy storage technologies. Reproduced by permission from American Chemical Society Z. Yang, J. Zhang, M.C. Kintner-Meyer, X. Lu, D. Choi, J.P. Lemmon, J. Liu, Chemical Reviews 111 (2011) 3577e3613. Copyright

The latest developments in battery technology have led to the development of flow batteries, which utilize features such as scalability and modularity in conventional electrochemical storage technologies. By storing the liquid electrolyte in a separate container outside the battery, they provide a better way to manage its energy capacity. If necessary, the electrolyte must be pumped into the battery containing the electrodes.

Therefore, this allows the system to have a large energy capacity independent of the power capacity of the battery module.

Further, advantages of VRFB are that they can operate over a wide range of power inputs and outputs; furthermore, VRFB can be completely discharged without damaging the battery [1], [8].

Beside the positive characteristics of the VRFB, electrochemical side reactions can occur during long-term operation leading to capacity fade due to diffusion, gas evolution, and air oxidation [9]. The capacity fade due to diffusion of vanadium ions through the membrane can simply be overcome by remixing the electrolyte in order to rebalance the ion concentrations [9].

Nevertheless, in terms of long-life cycle, the VRFB has an advantage due to the fact that the energy carrier, the electrolyte, can be restored and the peripheral components must be replaced after obsolescence. Over the last years, several VRFB models have been presented in the literature.

A detailed 2-D model of a single-cell battery based on mass, charge, and momentum laws is proposed by Shah et al. [10], to investigate the effects of variation ion concentration, electrolyte flow rate, and electrode porosity. This model is further extended to consider the evolution of oxygen and hydrogen [11], and to observe the effect of current density, electrode porosity, and local mass transfer coefficient on the cell performance [10]. Tang et al. [9] proposed a dynamic model of a single-cell battery to describe the capacity loss caused by diffusion and side reactions.

Such detailed models provide important insights for the development and improvement of the core components of VRFB, but they require more computational resources and may not be practical for long-term simulations at system level. At this level, models can be applied to optimize the battery design and fabrication

as the model presented in [12] or to focus more on the application of VRFB in interaction with other energy systems [13].The two other side reactions cause a permanent imbalance of the electrolyte, which requires chemical or electrochemical rebalancing methods to restore the capacity.

Different types of flow batteries are now available, such as redox batteries, non-membrane batteries and hybrid batteries [14].

As the name suggests, the redox battery is characterized by the simultaneous redox reactions occurring in the electrodes of the battery cells. Many redox batteries have been developed, such as iron-chromium flow batteries, vanadium flow batteries, zinc bromide flow batteries, etc.

The redox battery is characterized by the simultaneous redox reactions occurring in the electrodes of the battery cells. In this study, the vanadium redox battery (VRB) was chosen because it is the most promising of all long-life redox batteries and offers considerable energy capacity without any heating problems.

Tableau 1:General comparison of static battery, redox flow cells and fuel cells [8]

Electrochemical device	Site of reactants/products	Electrolyte conditions	Separator
Static battery	Active electrode material	Static and held within cell	Microporous polymer separator
Redox flow cell	Aqueous electrolytes in reservoirs	Electrolyte-recycles through the cell	Ion-exchange membrane (cationic or anionic)
Fuel cell	Gaseous or liquid fuel plus air	Solid polymer or ceramic acts as solid electrolyte within cell	Ion-exchange membrane polymer or ceramic

The advantages of redox flow cells can be summarized in four features: moderate cost, modularity, transportability and flexible operation. Due to their modular design its construction and maintenance costs could be the lowest of any of the storage systems mentioned above. The redox flow batteries are well-suited for transmission and distribution deferral applications, where batteries might be transported from substation to substation or load center in order to provide local capacity needed to defer expensive upgrades [8] .

Tableau 2:Advantages and disadvantages of storage systems compared to redox flow cells[8]

Battery energy storage system	Advantages	Disadvantages	Redox system
Conventional systems	Well-known technology Low maintenance Low size	Frequent maintenance Heavy High construction cost Not portable Expensive technology	Flooded lead-acid battery Valve-regulated lead-acid (VRLA)
Developmental systems	Transportability High energy (charging) efficiency Flexible operation	Thermal management Difficult maintenance	Sodium/sulfur battery Zinc/bromine redox flow cell
Redox flow cells	Low cost Modularity Transportability Flexible Operation High efficiency Large scale	Newer technology	Bromine/polysulfide redox flow cell Vanadium redox flow cell Iron/chromium redox flow cell Zinc/cerium redox flow cell

II. VANADIUM REDOX FLOW BATTERY (VRFB)

The vanadium redox flux (VRB) battery is an electrochemical energy storage system based on a reversible chemical reaction in a sealed electrolyte. VRB are essentially comprised of two key elements: the cell stacks, where chemical energy is converted to electricity in a reversible process, and the tanks of electrolytes where energy is stored [6].

It consists of two electrolyte tanks, containing sulfuric acid electrolyte with active vanadium species in different oxidation states: V_4 / V_5 redox couple (positive) and V_2 / V_3 redox couple (negative).

Both electrolytes are circulated through the cell stack by pumps. The stack consists of many cells, each of which contains two half-cells that are separated by a proton exchange membrane (PEM)[6].
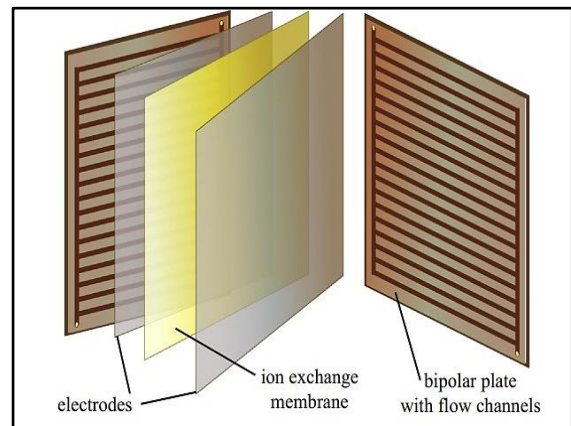

Figure 3:Typical configuration of a classical all-vanadium redox flow battery single cell [2]
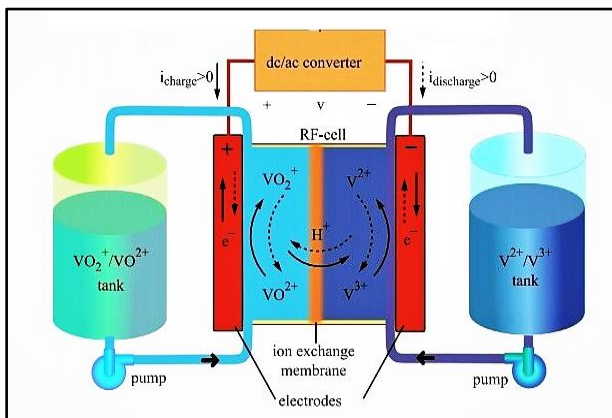

Figure 2:General Scheme of a Vanadium Redox Flow [2]

In the half-cells the electrochemical reactions take place on inert carbon felt polymer composite electrodes from which an external direct current is used, in order to charge or discharge the battery. During discharge, electrons are removed from the negative electrode electrolyte (anolyte) and transferred to the positive electrode electrolyte (positive electrolyte) via an external circuit.

The flow of electrons is reversed during charging. Reduction occurs in the anolyte, while oxidation occurs in the catholyte [15].

The nominal potential produced by a single cell is about 1.35 V, depending on the concentration of vanadium. The terminal voltage is obtained by connecting several batteries in series in a "cell". The energy available is related to the battery voltage and the current density established by the battery and the energy available depends solely on the supply of electrolyte charged in the battery. Therefore, the power rating and stored energy can be easily increased by adding or reducing the battery and the electrolyte reservoir, respectively.

III. MODELING OF VRFBS: A NEW MODEL OF THE VRB STACK

A. Electrical Equivalent model of VRFB

The charging and discharging of VRFB involves chemical reactions in positive and negative half cells where the four electro-active states of Vanadium (V^{2+}, V^{3+}, V^{4+}, V^{5+}) are reversibly exchanged through oxidation and reduction process. During charging in the positive side, the V^{4+} (Basically oxide VO_{2+}) is converted into V^{5+} (Basically Oxide VO_{2+}) by oxidation and in the negative side V^{3+} is converted into V^{2+} by reduction reaction. The whole process takes place by exchange of proton through ion exchange membrane and subsequent removal of water molecule.

To estimate the electrode potential the of the two sides, VRFB positive half-cell equilibrium potential and negative half-cell equilibrium potential are considered as E^{0+} = 1.182 V [30] and E^{0-} = -0.207 V [16] at SHE (Standard Hydrogen Electrode) [17].

Thus, the cell equilibrium potential becomes E^0 = 1.39 V [16] which is calculated by the difference between the equilibrium cell potentials of the two electrodes (positive and negative) expressed in Eq1:

$$E^0 = E^{0+} - E^{0-} \qquad (1)$$

In the Nernst equation, SOC is the initial State of Charge which is defined as the capacity of energy stored in the electrolytes divided by the energy rating, n is the number of cells in the stack,

- V equilibrium is equal to the cell voltage at 50% SOC,
- F is the Faraday constant with the value of 96485C/mole,
- R is the universal gas constant with the value of 8.3145J/(K. mole),
- T is the temperature in the Kelvin scale.

Both parameters $R_{Reaction}$ and $R_{Resistive}$ compose the internal losses, which electrically reflect reaction kinetics, mass transport resistance, membrane resistance, solution resistance, electrode resistance and bipolar plate resistance.

The parasitic losses are presented by a constant resistance $R_{fixedloss}$ and a controlled current source I pump, which stands for the power consumption of the re-circulation pump, system controller, and power loss from cell-stack by-pass.
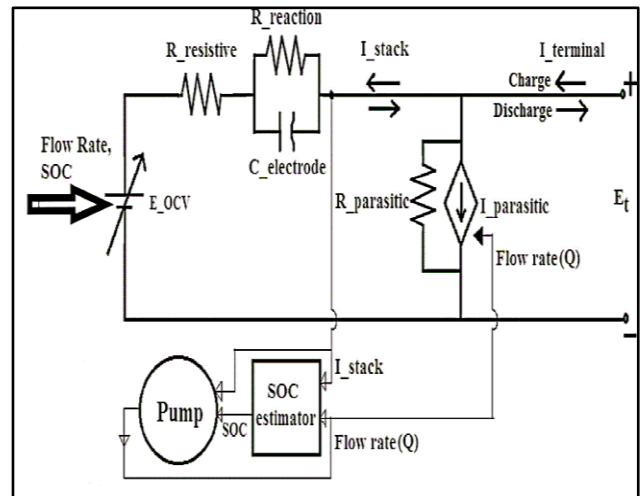

Figure 5: Faunctional schematic of the electrical equivalent model of a practical VRFB

In this model, the pump and the associated controller circuit losses (parasitic losses) are represented as a combination of controlled current source ($I_{Parasitic}$) and a shunt resistor ($R_{Parasitic}$) in the VRFB electrical equivalent model. Similarly, the self-discharge loss of VRFB is also represented in the model.

To understand the electrical equivalent circuit of a practical VRFB system, a schematic diagram is developed as shown in Fig. 5 where the electrical RC equivalent model is represented by typical Randles equivalent circuit. Based on the proposed schematic in Fig.5, an electrical characteristics model of VRFB system is developed in MATLAB/ Simulink environment as shown in Fig. 4.
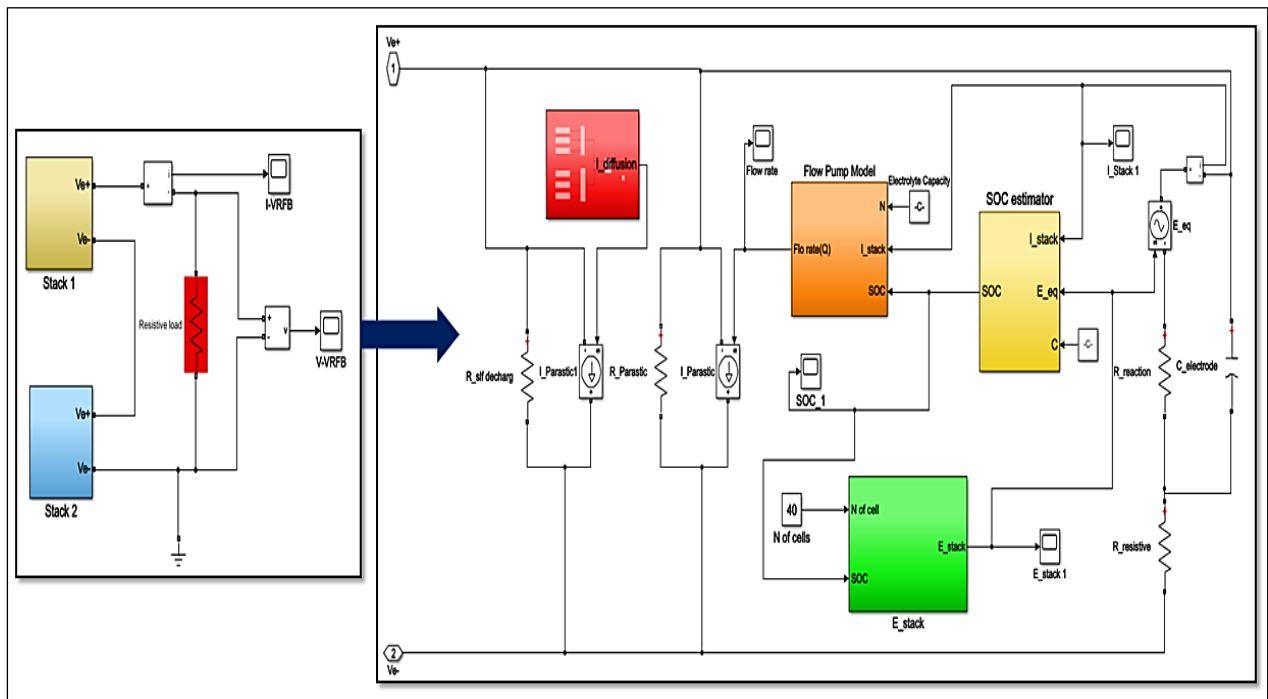

Figure 4: Generalised electrical characteristics model of a VRFB in MATLAB/Simulink

To analyze the whole model of the VRFB system it has been divided into three major subsystems namely

- E$_{Stack}$ Estimator
- SOC Estimator and Stack Voltage estimation
- Flow Pump model

The proposed model has been constructed based on the following assumptions:

- Positive and negative side electrolytes are in chemically balanced condition.
- The pumps are not operational during the period when the battery is in the open circuit mode.
- VRFB Stack temperature and electrolyte temperature are almost constant (29–31C).

B. VRFB storage modeling

The VRFB stores chemical energy and generates electrical energy through redox reactions between vanadium ions dissolved in the electrolyte. The most important feature of the VRFB is its modularity of power (Watt) and energy (Watt-hour), which are independent of each other, so that they can be expanded independently depending on the PV solar energy and load capacity.

1) E$_{Stack}$ Estimator

The basic idea of the VRFB stack estimation model is obtained from the Nernst potential equation. In equation (1) in section 1, the cell equilibrium potential was discussed on the basis of the two half-cell potentials (positive and negative).

To develop a model for estimating the open-circuit voltage of a battery, the equation Eq can be used. Calculate in more detail using the following equation (1).

In the positive electrode side:

$$E^+ = E^{0+} - \frac{RT}{F} \ln \left\{ \frac{[VO^{2+}]}{[VO_2^+][H^+]^2} \right\} \tag{2}$$

In the negative electrode side:

$$E^- = E^{0-} - \frac{RT}{F} \ln \left\{ \frac{[V^{2+}]}{[V^{3+}]} \right\} \tag{3}$$

Where:

E^+ = Positive electrode potential (Volts)

E^- = Negative electrode potential (Volts)

R = Universal gas constant (8.3144J K^{-1}. mol^{-1})

T = Ambient temperature (K)

$[VO^{2+}]$ = Concentration of VO^{2+} (mol.L^{-1})

$[VO_2^+]$ = Concentration of VO_2^+ (mol.L^{-1})

$[V^{2+}]$ = Concentration of V^{2+} (mol.L^{-1})

$[V^{3+}]$ = Concentration of V^{3+} (mol.L^{-1})

Now taking H^+ concentration to be constant (Corcuera et al. [18] have assumed [H$^+$] as 1 mol to eliminate its effect on the Nernst Potential).

According to the above assumptions, Eq (2) can be replaced by;

$$E^+ = E^{0+} - \frac{RT}{F} \ln \left\{ \frac{[VO^{2+}]}{[VO_2^+]} \right\} \tag{4}$$

Eq (2-4), the relation between Vanadium Concentration with the SOC is established to design a competitive model of cell equivalent voltage estimation.

During charging, the SOC increases with time and during discharging the reverse happens. Inside the positive half-cell the $[VO_2^+]$ increases during charging whereas $[VO^{2+}]$ reduces due to oxidation and inside the negative half cell the $[V^{2+}]$ increases during charging whereas $[V^{3+}]$ reduces due to reduction process.

During the discharge process, an inverse phenomenon occurs inside the two half-cells. Therefore, we can deduce the following relationship from the above phenomenon[18], [19] :

- Positive Half Cell:
$$[VO_2^+] = K * SOC[V] \text{ and } [VO^{2+}] = K * (1 - SOC)[V] \tag{5}$$

- Negative Half Cell:
$$[V^{2+}] = K * SOC[V] \text{ and } [V^{3+}] = K * (1 - SOC)[V] \tag{6}$$

Where:

k is proportionality constant and [V] is the total Vanadium concentration (mol.L^{-1})

From the Eqs. (5) and (6) we can finally establish the mathematical relationship between SOC and the equivalent cell Potential E$_{Stack}$:

$$E_{cell,eq} = E^+ - E^- \tag{7}$$

$$E_{cell,eq} = E^{0+} - \frac{RT}{F} \ln \left\{ \frac{1 - SOC}{SOC} \right\} - E^{0-} - \frac{RT}{F} \ln \left\{ \frac{SOC}{1 - SOC} \right\} \tag{8}$$

$$E_{cell,eq} = E^{0+} - E^{0-} + \frac{2RT}{F} \ln \left\{ \frac{SOC}{1 - SOC} \right\} \tag{9}$$

Then the VRFB stack open circuit potential is calculated by:

$$E_{stack} = n * \left\{ E_{cell,eq(at\ 50\%\ SOC)} + \frac{2RT}{F} \ln \left(\frac{SOC}{1 - SOC} \right) \right\} \tag{10}$$

Where:

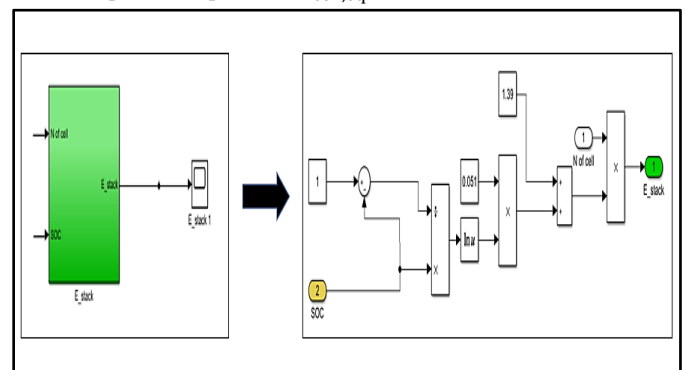The cell equilibrium potential E$_{cell,eq}$= 1.39 V as mentioned in [18].

Figure 6: E_{stack} Schematics in Matlab/Simulink

2) Flow Pump model

The most important parameter to model the flow pump is the electrolyte flow rate (Q). The flow rate again depends on three factors namely Stack current (I$_{Stack}$), SOC (estimation model will be discussed) and electrolyte capacity (N).

The flow rate is directly proportional to Stack current (I_{Stack}) and inversely proportional to SOC and electrolyte capacity (N). The mathematical expression of flow rate (Q) based on which the pump has been modelled is given in Eq. (2):

$$Q = \frac{I_{Stack}}{N * SOC} \text{ cm}^3 \text{sec}^{-1} \qquad (11)$$

The electrolyte capacity (N) is also dependent upon some chemical parameters [20]expressed as :

$$N = n_e * c * F \text{ A s cm}^{-3} \qquad (12)$$

Where:

n_e = No. of electron transferred/mol

c = Vanadium concentration in the electrolyte (mol L^{-1})

F = Faraday's constant (96,485 C mol^{-1})

Here the total vanadium concentration (mol L^{-1}) is assumed to be constant as 1.6 mol L^{-1} for simulation.

Considering the pressure drop in flow pipes and the stack, head loss and finally the mechanical power consumption of the pump is calculated based on the equations and assumptions of Zhang et al.

The pump power loss and the pump controller circuit [21] losses are represented by a controlled current source ($I_{Parasitic}$) and a shunt resistance ($R_{Parasitic}$).

The pump internal resistance and the auxiliary control circuit resistance are clubbed into a single resistance which is approximated as 13.889V based on the literature of Barote et al. [22], [23].

The relation between the variables ($I_{Parasitic}$ with I_{stack} and SOC) involved in the flow pump model subsystem is shown in Fig. 4.
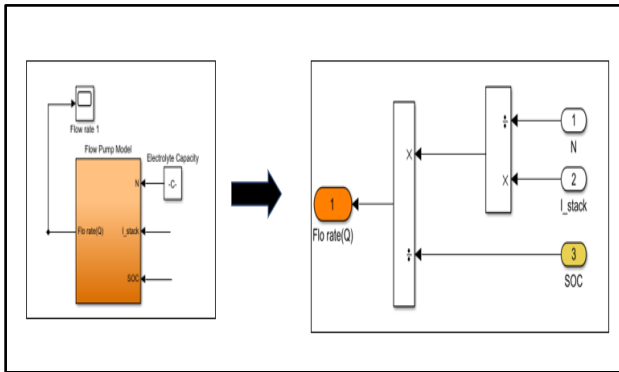

Figure 7:Flow Pump Model Schematic in Matlab/Simulink

3) State of Charge model (SOC)

The State of Charge of the Battery VRF is estimated by dynamically updating its value for every time step. The SOC of the system can be defined as seen in Eq. 13

$$SOC = \frac{\text{Current Energy in Battery}}{\text{Total Energy Capacity}} \qquad (13)$$

SOC is changed based on the power delivered/absorbed by the cell stack. So, each time step the SOC is tracked it can use the previous SOC obtained to determine the future SOC value. The change in SOC is implemented as seen in [14, Eq. (14-16)].

$$SOC(t + 1) = SOC(t) + \Delta SOC \qquad (14)$$

$$\Delta SOC = \frac{\Delta E}{E_{capacity}} = \frac{I_{stack} * V_{stack} * t}{P_{rating} * t_{rating}} \qquad (15)$$

$$\Delta SOC = I_{stack} * V_{stack} * C \qquad (16)$$

The inputs are two variable parameters (I_{stack}; V_{stack}) and one constant block (C). With the help of a discrete time–integrator block in Matlab the SOC of the battery is accumulated and thus it is computed at each cycle based on the previous SOC, depending on the input values.

An important issue in battery modeling is transient behavior. The ability of the system to respond quickly to fast changes is especially important for power smoothing applications. In a VRB battery, the transient effects are related to electrode capacitance
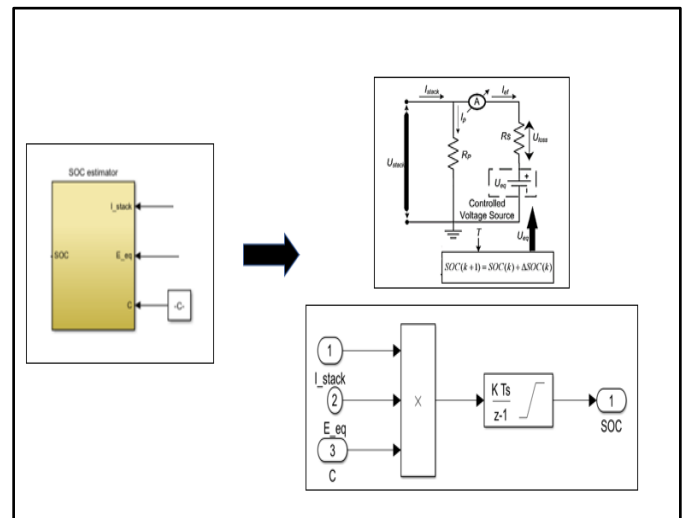

Figure 8:SOC Estimator Schematics in Matlab/Simulink

IV. SYSTEM CONFIGURATION

A. Model description

The proposed system model includes three main subsystems: solar PV panels, MPPT controller and DC-DC boost converter, VRFB storage.

1) Assumptions for Vanadium Redox Flow Battery

- Energy storage system has capacity of 10 kWh. The system contains two stacks with power rating of 1 kW each. Stack output voltage is 48 V
- Single cell voltage is 1.0 V, current density is at 0.1 A cm^{-1}, the bipolar plate thickness is 0.6 cm, and the end plate thickness is 10 cm.
- The cell voltage-current relationship is based on Nernst equation and the cell internal resistance. No activation over-potential and concentration over-potential are taken into consideration.

2) Battery Power Density and Energy Density

First, the stack volume was calculated. We assume a 10 kWh energy storage battery contains two stacks. Two stacks (N_{stack}=2) have power rating (P_{stack}) of 1 kW. Voltage of each stack (E_{stack}) is 48 V. Two stacks are connected in series. The stack current (I_{stack}) is:

$$I_{stack} = \frac{P_{stack}}{E_{stack} * N_{stack}} = \frac{1000}{48 * 2} = 10.4A \qquad (17)$$

If the cell voltage of a single cell (E_{cell}l) is 1.0 V, then the number of cell (N_{cell}) in a stack to produce stack voltage of 48 V is:

$$N_{cell} = \frac{E_{stack}}{E_{cell}} = 48 \qquad (18)$$

We assume the thickness of a bipolar plate is 0.6 cm and the thickness of endplate is 10 cm, then the stack length L_{stack} is:

$$L_{stack} = [L_{bipolar} * (N_{cell} + 1)] \qquad (19)$$
$$+ (2 * L_{endplate})$$

$$L_{stack} = 50 \ cm \qquad (20)$$

If the cell is operated at current density (i_{cell}) of 0.1 A cm^{-2}, then the cell cross section area (A_{stack}) is:

$$A_{stack} = \frac{I_{stack}}{i_{cell}} * 1.4 = 146 \ cm^2 \qquad (21)$$

Stack volume (V_{stack}) is:

$$V_{stack} = L_{stack} * A_{stack} = 7 \ Liter \qquad (22)$$

Total Volume of two stacks is 14 Liters.

The volume of electrolyte storage is calculated as follows. For a 100% discharge- charge battery, the volume of electrolyte ($V_{electrolyte}$) for positive electrode or for negative electrode can be calculated from equation (23).

$$C * V_{electrolyte} = \frac{I_{stack} * t_{charge}}{n_{rxn} * F} \qquad (23)$$

Here "C" is the reactant concentration, "t_{charge} " is the charge time in seconds, "n_{rxn} " is the equivalent of reaction (n_{rxn}=1), and "F" is Faraday constant (96500 Coulomb/equivalent). For C = 2 M, the volume of electrolyte needed for 10 hr charge-discharge is 187 liters and the total electrolyte volume is 374 liters.

The volume of the stack is about 3.6% of the system. Majority of the battery volume is electrolyte. For a 10 kWh energy storage and 1 kW stack, the stack power density is 69 W/L and battery power density is 2.6 W/L. The battery energy density is 26 Wh/L.

3) PV PLANTS DESCRIPTION

A. Meteorological conditions

Fig. 9 shows the monthly ambient temperature and the monthly horizontal solar radiation. The reported average annual ambient temperature is 19.11°C. The recorded maximum value of temperature is 29.21 in July and the lowest value was 9.24°C in January. The monthly global horizontal irradiance ranged from 98.9 kWh/m^2 in January to 240.4 kWh/m^2 in July.
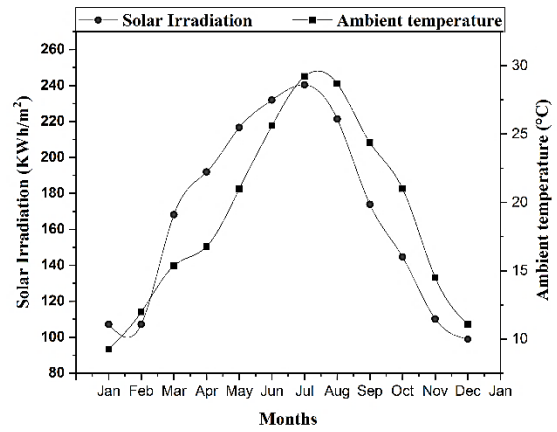

Figure 9: The monthly ambient temperature and horizontal solar radiation

The photovoltaic system was installed on the rooftop (Fig.10) of the Faculty of Science and Technology, Beni Mellal, Morocco. It consisted of three mini-stations of 2kWp photovoltaic for each one, distinguished by the three silicon technologies: Monocrystalline (mc-si), Polycrystalline (pc-si) and Amorphous (a-si). Each mini-station of both monocrystalline and polycrystalline types formed by eight panels of Sunmodule plus SW 255 Wp from Solarworld. The modules, which are included 60 solar cells connected in series, have a yield of 15% under standard test conditions [24].

Every string is connected to the 3-phase Sunny Boy 2500HF inverter. The Amorphous Silicon mini-station consists of 12 panels of NEXPOWER NT_155AF 155 Wp forming two strings joined in parallel. Each string is formed by connecting 6 modules in series. Both strings are linked to a 3-phase Sunny Boy 2500HF inverter. The unshaded modules were fixed with a tilt angle of 30°, facing south at an azimuth angle of 0°. [25]

More details can be illustrated in Table.3

Figure 10:The three PV plant

Tableau 3:Electrical characteristics

Modules	mc-si	pc-si	a-si
Module nominal power (W)	255	255	155
Module nominal open circuit voltage (V)	37.8	38	85.5
Module nominal voltage at maximum power (V)	31.4	30.9	65.2
Module nominal short circuit current (A)	8.66	8.88	2.56
Module nominal current at maximum power (A)	8.15	8.32	2.38
Temperature coefficient of power (per K)	-0.450%	-0.410%	-0.280%
Temperature coefficient open circuit voltage (per K)	-0.300%	-0.310%	-0.320%
Temperature coefficient short circuit current	0.004%	0.051%	0.070%

Tableau 4: Geographic coordinates, mean temperature and global horizontal irradiation

	Beni Mellal
Latitude	32°20' North
Longitude	6°21' West
Average temperature	23,47
Overall horizontal irradiation (kWh/m² /year)	2392,87

To extract maximum power from the solar PV array, Perturb and Observe algorithm is used for its simplicity in implementation. The algorithm performance is tested under a practical irradiance profile. A suitable DC-DC boost converter is designed in MATLAB/Simulink to track the maximum power from the solar PV array. The aim of maintaining high dc link voltage at the PCC (point of common coupling) is to minimize losses. The MATLAB/Simulink model of the DC-DC boost converter is shown in figure 11.
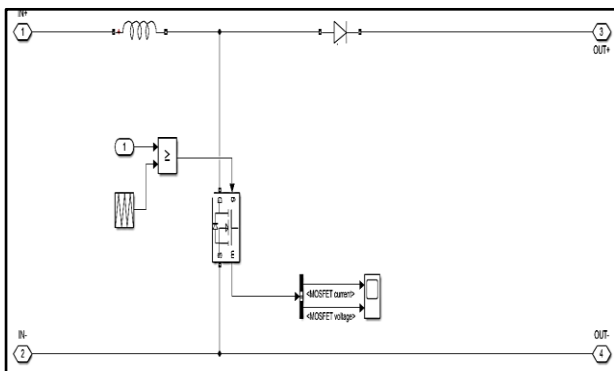

Figure 11:MATLAB/Simulink model of DC-DC boost converter

V. SIMULATION RESULTS AND DISCUSSION

The initial value of SOC of the battery was set to 90% as shown in figure 12. Since the battery is discharging through a 2.6 kW resistive load the SOC was dropped from 0.9 (initial set value) to 0.898 in a time interval of 2 sec.
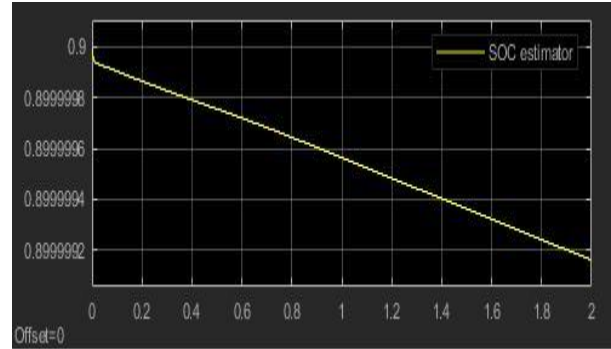

Figure 12:SOC of the VRF battery

At 90% SOC, the calculated stack1 voltage of the VRF battery from Eq. 10 was found to be 30.04 V which is same as shown in figure 8 and the stack1 voltage is discharged to a value of 30.01 V at 0.898 SOC as from the Eq.10.
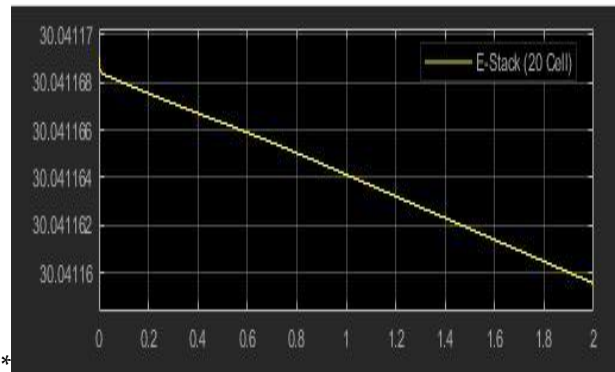

Figure 13: Stack Voltage of VRF Battery

The output voltage from the VRF battery is shown in figure 14. Its average value was found to be 28.217V.
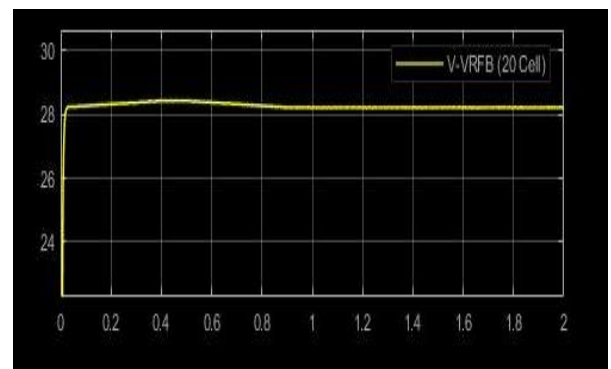

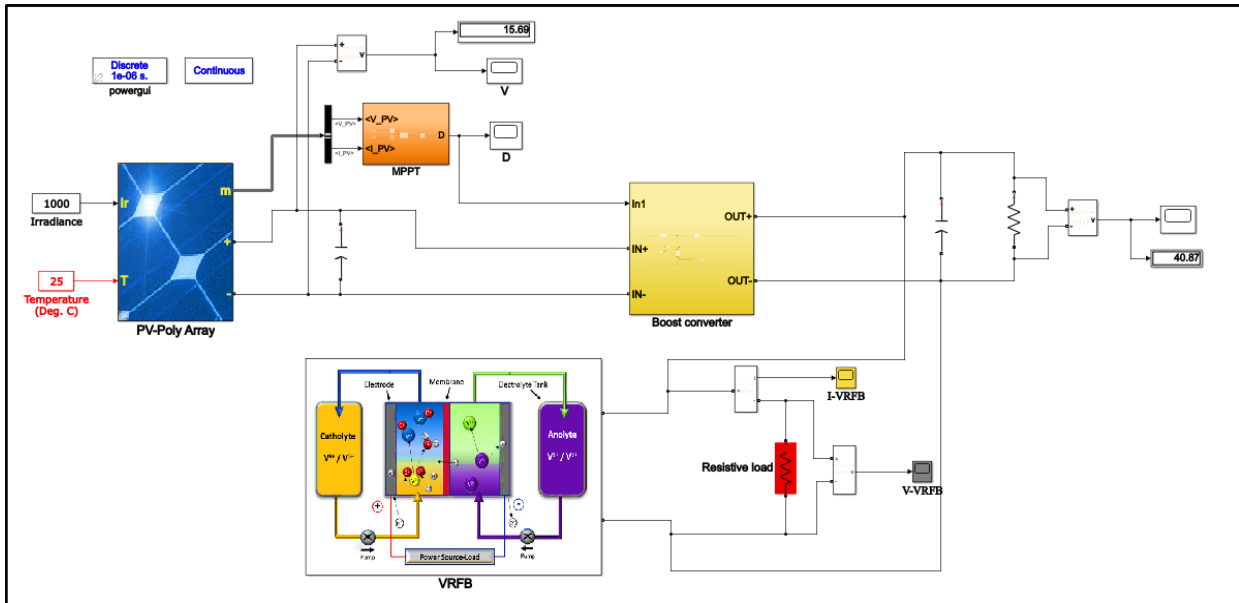**Figure 14:**Output voltage of the VRF Battery

Figure 15:Schematic Schematic of the proposed system in MATLAB/Simulink

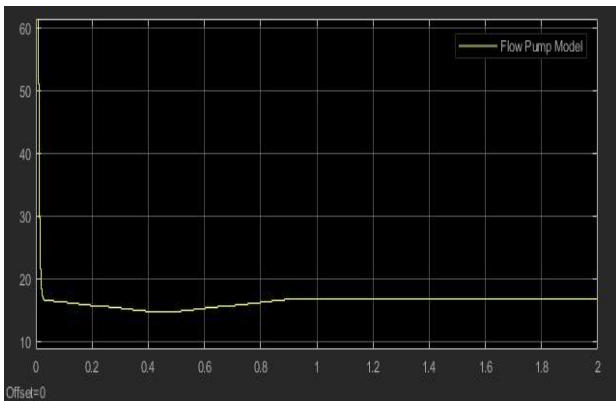**Figure 16**:Flow rate pump

From the flow rate calculated from the flow pump model, the current absorbed by the current control source (I_parasitic) of stack 1 was found to be 0.23 A (calculated from Eq. 11) and the value of flow rate is 16.98 as shown in figure 16.
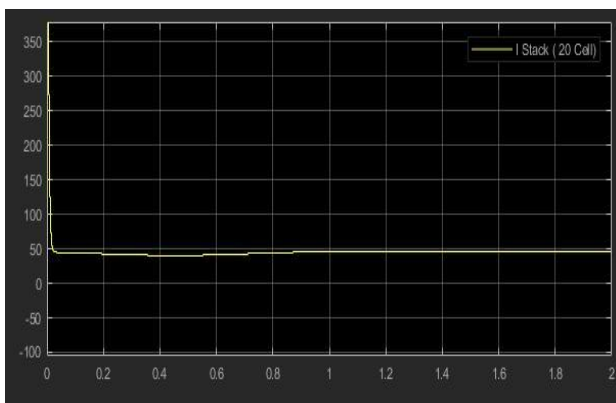

Figure 17:Load current of the VRF Battery

The VRF battery is discharged to supply 2.6kW power to the resistive load with a load current of 45.7A as shown in figure 17.

VI. CONCLUSION

The proposed work has demonstrated the performance of VRFB storage. The VRFB storage state of charge (SOC) is kept within an operating limit of 10% to 90% to avoid deep discharge and thus lengthening the battery lifetime.

This paper has successfully established a VRFB model in Matlab / Simulink environment considering the influence of flow rate, flow pump loss and parasitic loss. A SOC estimation technique for dynamic updating of the VRFB is proposed. The simulation results show that the VRFB can deliver 2.6 kW - 3.4 kW of active power to the resistive loads with a deviation of 0.063%. The simulated value matches the calculated value. The discharge characteristics of the VRFB, such as a decrease in SOC and the battery voltage transition over time, were also observed.

Resistive Load	N of Cell	I VRFB	V VRFB	E Stack	I Stack	Flow Rate pump
2.6 kW	10	14.8	14.23	15.02	19.76	7.318
	20	29.34	28.21	30.04	45.7	16.93
	30	43.91	42.23	45.06	70.9	26.26
	40	58.49	56.24	60.08	96.09	35.59
	50	73.06	70.25	75.1	121.3	44.92
3.4 kW	10	18.99	13.97	15.02	26.38	9.77
	20	37.66	27.69	30.04	58.83	21.79
	30	56.36	41.44	45.06	90.55	33.54
	40	75.06	55.19	60.08	122.3	45.28
	50	93.76	68.94	75.1	154	57.03

VIII. REFERENCES

[1] M. H. Chakrabarti, S. A. Hajimolana, F. S. Mjalli, M. Saleem, and I. Mustafa, "Redox Flow Battery for Energy Storage," *Arab. J. Sci. Eng.*, vol. 38, no. 4, pp. 723–739, 2013.

[2] P. Alotto, M. Guarnieri, and F. Moro, "Redox flow batteries for the storage of renewable energy: A review," *Renew. Sustain. Energy Rev.*, vol. 29, pp. 325–335, 2014.

[3] F. T. Wandschneider *et al.*, "Model of a vanadium redox flow battery with an anion exchange membrane and a Larminie-correction," *J. Power Sources*, vol. 272, pp. 436–447, 2014.

[4] M. H. Li, T. Funaki, and T. Hikihara, "A study of output terminal voltage modeling for redox flow battery based on charge and discharge experiments," *Fourth Power Convers. Conf. PCC-NAGOYA 2007 - Conf. Proc.*, pp. 221–225, 2007.

[5] R. D'Agostino, L. Baumann, A. Damiano, and E. Boggasch, "A Vanadium-Redox-Flow-Battery Model for Evaluation of Distributed Storage Implementation in Residential Energy Systems," *IEEE Trans. Energy Convers.*, vol. 30, no. 2, pp. 421–430, 2015.

[6] L. J. Ontiveros and P. E. Mercado, "Modeling of a Vanadium Redox Flow Battery for power system dynamic studies," *Int. J. Hydrogen Energy*, vol. 39, no. 16, pp. 8720–8727, 2014.

[7] A. H. Fathima and K. Palanismay, "Modeling and Operation of a Vanadium Redox Flow Battery for PV Applications," *Energy Procedia*, vol. 117, pp. 607–614, 2017.

[8] C. Ponce de León, A. Frías-Ferrer, J. González-García, D. A. Szánto, and F. C. Walsh, "Redox flow cells for energy conversion," *J. Power Sources*, vol. 160, no. 1, pp. 716–732, 2006.

[9] A. Tang, J. Bao, and M. Skyllas-Kazacos, "Dynamic modelling of the effects of ion diffusion and side reactions on the capacity loss for vanadium redox flow battery," *J. Power Sources*, vol. 196, no. 24, pp. 10737–10747, 2011.

[10] N. Gurieff, D. F. Keogh, V. Timchenko, and C. Menictas, "Enhanced reactant distribution in redox flow cells," *Molecules*, vol. 24, no. 21, 2019.

[11] A. A. Shah, H. Al-Fetlawi, and F. C. Walsh, "Dynamic modelling of hydrogen evolution effects in the all-vanadium redox flow battery," *Electrochim. Acta*, vol. 55, no. 3, pp. 1125–1139, 2010.

[12] A. Tang, J. Bao, and M. Skyllas-Kazacos, "Thermal modelling of battery configuration and self-discharge reactions in vanadium redox flow battery," *J. Power Sources*, vol. 216, pp. 489–501, 2012.

[13] B. Turker, S. Arroyo Klein, E. M. Hammer, B. Lenz, and L. Komsiyska, "Modeling a vanadium redox flow battery system for large scale applications," *Energy Convers. Manag.*, vol. 66, pp. 26–32, 2013.

[14] A. Z. Weber, M. M. Mench, J. P. Meyers, P. N. Ross, J. T. Gostick, and Q. Liu, "Redox flow batteries: A review," *J. Appl. Electrochem.*, vol. 41, no. 10, pp. 1137–1164, 2011.

[15] C. Blanc and A. Rufer, "Optimization of the operating point of a vanadium redox flow battery," *2009 IEEE Energy Convers. Congr. Expo. ECCE 2009*, pp. 2600–2605, 2009.

[16] M. Skyllas-Kazacos and M. Kazacos, "State of charge monitoring methods for vanadium redox flow battery control," *J. Power Sources*, vol. 196, no. 20, pp. 8822–8827, 2011.

[17] A. Bhattacharjee and H. Saha, "Design and experimental validation of a generalised electrical equivalent model of Vanadium Redox Flow Battery for interfacing with renewable energy sources," *J. Energy Storage*, vol. 13, pp. 220–232, Oct. 2017.

[18] S. Corcuera and M. Skyllas-Kazacos, "State-of-Charge Monitoring and Electrolyte Rebalancing Methods for the Vanadium Redox Flow Battery," *Eur. Chem. Bull.*, vol. 1, no. 12, pp. 511–519, 2012.

[19] C. Blanc and A. Rufer, "Understanding the Vanadium Redox Flow Batteries," *Paths to Sustain. Energy*, no. November 2010, 2010.

[20] C. Blanc, "Modeling of a vanadium redox flow battery electricity storage system," Jan. 2009.

[21] T. A. Nguyen, M. L. Crow, and A. C. Elmore, "Optimal sizing of a vanadium redox battery system for microgrid systems," *IEEE Trans. Sustain. Energy*, vol. 6, no. 3, pp. 729–737, 2015.

[22] C. Blanc *et al.*, "Modeling and Operation of a Vanadium Redox Flow Battery for PV Applications," *J. Power Sources*, vol. 13, no. 2, pp. 607–614, 2015.

[23] L. Barote and C. Marinescu, "A new control method for VRB SOC estimation in stand-alone wind energy systems BT - 2009 International Conference on Clean Electrical Power, ICCEP 2009, June 9, 2009 - June 11, 2009," no. 22134, pp. 253–257, 2009.

[24] M. Adar, Y. Najih, M. Gouskir, A. Chebak, M. Mabrouki, and A. Bennouna, "Three PV plants performance analysis using the principal component analysis method," *Energy*, vol. 207, 2020.

[25] M. Adar, H. Bazine, Y. Najih, C. Bahanni, M. Mabrouki, and A. Chebak, "Simulation study of three PV systems," *Proc. 2018 6th Int. Renew. Sustain. Energy Conf. IRSEC 2018*, 2018.